Ultra Scientist Vol. 28(2)A, 111-127 (2016). ISSN 2231-3478 (Print)
www.ultrascientist.org 2319-8052 (Online)

Analysis of Joule heating and Radiation on Hydromagnetic Peristaltic flow with porous medium through a coaxial asymmetric Vertical Inclined Tapered Channel

Sk. ABZAL[*1], S.VIJAYA KUMAR VARMA[2] and S. RAVI KUMAR[3]

[1]Department of Mathematics, NBKR Institute of Science and Technology (Autonomous), Vidyanagar, SPSR Nellore,Andhra Pradesh (India)
[2]Department of Mathematics, Sri Venkateswara University, Tirupati, Andhra Pradesh (India)
[3]Department of Mathematics NBKR Institute of Science and Technology (Autonomous), Vidyanagar, SPSR Nellore,Andhra Pradesh, India.
Corresponding author email:abbuoct23@gmail.com

(Acceptance Date 19th June, 2016)

Abstract

The aim of the present attempt was to investigate ananalysis of joule heating and radiation on hydromagnetic peristalticflow with porous medium through a coaxial asymmetric vertical inclined tapered channel. The Mathematical modeling is investigated by utilizing long wavelength and low Reynolds number assumptions. Analytical solutions are obtained for the axial velocity, pressure gradient, temperature and heat transfer coefficient. The effects of Hartmann number, porosity parameter, volumetric flow rate, radiation parameter, non- uniform parameter, gravitational parameter, shift angle, Prandtl number, Brinkman number, heat source/sink parameter on axial velocity characteristics, pressure gradient characteristics, temperature characteristics and heat transfer coefficient characteristics are presented graphically and discussed in detail.

Key words: Joule heating, radiation parameter, inclined channel, tapered channel, MHD.

1. Introduction

The peristaltic flow of a fluid is very important for medical diagnosis and it has many clinical applications. These applications are swallowing of food bolus through the esophagus,

the urine transport from a kidney to the bladder, the movement of chime in the tract, the transport of lymph in the lymphatic vessels and the vasomotion of small blood vessel. The flow of non-Newtonian fluids also has benefit to the field environmental engineering, chemical and biomedical. Furthermore, the peristaltic pump is found in many applications of medicine, engineering and water waste. That is dialysis machine, a heart-lung machine, infusion pump, concrete pump, sewage sludge and etc. Magnetohydrodynamics deals with the study of motion of an electrically conducting fluid in presence of an applied magnetic field. When a conducting fluid moves through a magnetic field, electric currents are induced in the fluid. The magnetic field exerts a force known as the Lorentz force as a result the flow field is modified. Solid or fluid material moving in a magnetic field experiences an electromagnetic force. If the material is electrically conducting and a current path is available, electric current ensue. Alternatively, currents may be induced by change of the magnetic field with time and also study of flow through porous medium has received much attention in recent years because of its application in bio-physical and hydrological problem, industrial, particularly in nuclear, petroleum and chemical industries. The role played by porous medium in the study of the flow of blood and other fluids and electro-osmosis. This study is also useful to understand the mechanism of transfer heat from the deep interior of the earth to a shallow depth in the geothermal regions which are of vital importance in the present day grave power crisis. The study of behavior of fluid saturated porous media is known as Poromechanics.

LATHAM[1] made initial effort regarding peristaltic mechanism of viscous fluids. The primary mathematical models of peristalsis obtained by a train of sinusoidal waves in an infinitely long symmetric channel or tube were introduced by Fung and Yih[2] and Shapiro *et al.*[3]. Peristaltic flow of a Newtonian fluid in an asymmetric channel was described by Mishra and Ramachandra Rao[4]. In another attempt, Influence of convective conditions in radiative peristaltic flow of pseudoplastic nanofluid in a tapered asymmetric channel has discussed by T.Hayat *et al.*[5]. F. M. Abbasi *et al.*[6] presented a theoretical study on Numerical Analysis for Peristaltic Motion of MHD Eyring-Prandtl Fluid in an Inclined Symmetric Cannel with Inclined Magnetic Field. Some pertinent studies on the present topic can be found from the list of Refs. Such as Kh. S. Mekheimer[7], J.C. Misra, S. Maiti, G.C. Shit[8], M.H. Haroun[9], N.S. Akbar *et al.*[10], B.C. Sarkar *et al.*[11], Ravikumar [12-14].

In general heat transfer, play a vital role in MHD flows. When a fluid is at a different temperature from that of its surroundings, the thermal energy transfers from high-temperature region to low temperature region until the fluid and the surroundings attain thermal equilibrium. This is called heat transfer or heat exchange. Apart from this, there are many industrial, chemical engineering processes, Automotive Engineering, Thermal Insulations, Thermal Engineering of electronic devices and system, Material Processing, Power Plant Engineering, Bio-hear Transfer, Aerospace Technology, *etc*. Kabir, K. H. *et al.*[15] presented a theoretical study on effects of stress work on MHD natural convection flow along a vertical wavy surface with Joule heating. T. Hayat *et al.*[16]

have conferred the characteristics of convective heat transfer in the MHD peristalsis of Carreau fluid with Joule heating. F.M. Abbasi *et al.*[17] discussed on effects of inclined magnetic field and Joule heating in mixed convective peristaltic transport of non-Newtonian fluids. Recently, Ravi Kumar[18] investigated on Analysis of Heat Transfer on MHD Peristaltic Blood Flow with Porous Medium through Coaxial Vertical Tapered Asymmetric Channel with Radiation – Blood Flow Study. Some more works on this topic can be seen in (S. Nadeem and Noreen Sher Akbar[19], T. Hayat *et al.*[20], K. Vajravelu *et al.*[21], S. Srinivas and M. Kothandapani[22], T. Hayat *et al.*[23], .O. U. Mehmood *et al.*[24], Musharafa Saleem and Aun Haider[25], G. Radhakrishnamacharya, Ch. Srinivasulu[26], K. Vajravelu *et al.*[27], K. Ramesh, M. Devakar[28], M Kothandapani *et al.*[29] and Sk Abzal *et al.*[30]).

2. *Formulation of the problem :*

The model simulates the peristaltic transport of a viscous fluid through an infinite two-dimensional asymmetric vertical tapered channel through the porous medium. Asymmetry in the flow is due to the propagation of peristaltic waves of different amplitudes and phase on the channel walls. We assume that the fluid is subject to a constant transverse magnetic field B_0. The flow is generated by sinusoidal wave trains propagating with steady speed c along the tapered asymmetric channel walls[31].

The geometry of the wall surface is defined as

$$Y = H_2 = b + m'X + d\sin\left[\frac{2\pi}{\lambda}(X - ct)\right] \quad (2.1)$$

$$Y = H_1 = -b - m'X - d\sin\left[\frac{2\pi}{\lambda}(X - ct) + \phi\right] \quad (2.2)$$

Where b is the half-width of the channel, d is the wave amplitude, c is the phase speed of the wave and m' ($(m' << 1)$ is the non-uniform parameter, λ is the wavelength, t is the time and X is the direction of wave propagation. The phase difference ϕ varies in the range $0 \le \phi \le \pi$, $\phi = 0$ corresponds to symmetric channel with waves out of phase and further b, d and ϕ satisfy the following conditions for the divergent channel at the inlet $d\cos(\frac{\phi}{2}) \le b$

It is assumed that the left wall of the channel is maintained at temperature T_0 while the right wall has temperature T_1.

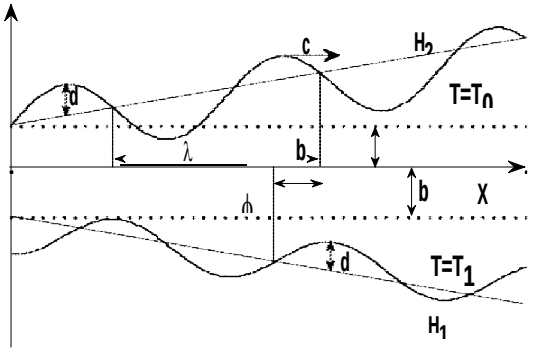

Fig. 1 Schematic diagram of the physicalmodel

The equations governing the motion for the present problem prescribed by
The continuity equation is

$$\frac{\partial u}{\partial x} + \frac{\partial v}{\partial y} = 0 \quad (2.3)$$

The movement equations are

$$\rho\left[u\frac{\partial u}{\partial x}+v\frac{\partial u}{\partial y}\right]=-\frac{\partial p}{\partial x}+\mu\left[\frac{\partial^2 u}{\partial x^2}+\frac{\partial^2 u}{\partial y^2}\right]-$$

$$\left[\sigma B_0^{\,2}\right](u+c)-\left[\frac{\mu}{k_1}\right](u+c)+\rho g\sin\alpha \quad (2.4)$$

$$\rho\left[u\frac{\partial v}{\partial x}+v\frac{\partial v}{\partial y}\right]=-\frac{\partial p}{\partial y}+\mu\left[\frac{\partial^2 v}{\partial x^2}+\frac{\partial^2 v}{\partial y^2}\right]-$$

$$\left[\sigma B_0^{\,2}\right]v-\left[\frac{\mu}{k_1}\right]v-\rho g\cos\alpha \quad (2.5)$$

The energy equation is

$$\rho C_p\left[u\frac{\partial}{\partial x}+v\frac{\partial}{\partial y}\right]T=k\left[\frac{\partial^2}{\partial x^2}+\frac{\partial^2}{\partial y^2}\right]T+$$

$$Q_0+\sigma B_0^{\,2}u^2-\frac{\partial q}{\partial y} \quad (2.6)$$

u and v are the velocity components in the corresponding coordinates, k_1 is the permeability of the porous medium, ρ is the density of the fluid, p is the fluid pressure, k is the thermal conductivity, μ is the coefficient of the viscosity, Q_0 is the constant heat addition/ absorption, C_p is the specific heat at constant pressure, σ is the electrical conductivity,g is the acceleration due to gravity and T is the temperature of the fluid.

The relative boundary conditions are

$\overline{U}=0$, $\overline{T}=T_0$ at $\overline{Y}=\overline{H}_1$

$\overline{U}=0$, $\overline{T}=T_1$ at $\overline{Y}=\overline{H}_2$

The radioactive heat flux (Cogley *et al.*[31]) is given by

$$\frac{\partial q}{\partial y}=4\alpha^2(T_0-T_1) \quad (2.7)$$

here α is the mean radiation absorption coefficient.

Introducing a wave frame (x, y) moving with velocity c away from the fixed frame (X, Y) by the transformation

$x = X-ct$, $y = Y$, $u = U-c$, $v = V$ and

$p(x) = P(X,t)$ (2.8)

Introducing the following non-dimensional quantities:

$$\bar{x}=\frac{x}{\lambda}\quad \bar{y}=\frac{y}{b}\quad \bar{t}=\frac{ct}{\lambda}\quad \bar{u}=\frac{u}{c}\quad \bar{v}=\frac{v}{c\delta}$$

$$h_1=\frac{H_1}{b}\quad h_2=\frac{H_2}{b}\quad p=\frac{b^2 p}{c\lambda\mu}\quad \theta=\frac{T-T_0}{T_1-T_0}\quad \delta=\frac{b}{\lambda}$$

$$\mathrm{Re}=\frac{\rho c b}{\mu}\quad N^2=\frac{4\alpha^2 d_1^{\,2}}{k}\quad \varepsilon=\frac{d}{b}\quad \eta=\frac{\rho a_0^{\,2} g}{\mu c}$$

$$\eta_1=\frac{\rho a_0^{\,3} g}{\lambda\mu c} \quad (2.9)$$

where $\varepsilon=\frac{d}{b}$ is the non-dimensional amplitude of channel $\delta=\frac{b}{\lambda}$, is the wave number, $k_1=\frac{\lambda m'}{b}$ is the non - uniform parameter , Re is the Reynolds number, M is the Hartman number $K=\frac{k}{b^2}$, Permeability parameter, Pr is the Prandtl number, E_c is the Eckert number, γ is the heat source/sink parameter, B_r (= E_cP_r) is the Brinkman number, η and η_1 are gravitational parameters and N^2 is the radiation parameter.

3. Solution of the problem :

In view of the above transformations (2.8) and non-dimensional variables (2.9), equations

(2.3-2.6) are reduced to the following non-dimensional form after dropping the bars

$$\mathrm{Re}\,\delta\left[u\frac{\partial u}{\partial x}+v\frac{\partial u}{\partial y}\right]=$$

$$\left(-\frac{\partial p}{\partial x}+\delta^2\frac{\partial^2 u}{\partial x^2}+\frac{\partial^2 u}{\partial y^2}-Au-A+\eta\sin\alpha\right)\quad(3.1)$$

$$\mathrm{Re}\,\delta^3\left[u\frac{\partial v}{\partial x}+v\frac{\partial v}{\partial y}\right]=\left(-\frac{\partial p}{\partial y}+\delta^4\frac{\partial^2 v}{\partial x^2}+\delta^2\frac{\partial^2 v}{\partial y^2}-\right.$$

$$\left.M^2\delta^2 v-\delta^2\frac{1}{Da}v-\eta_1\cos\alpha\right)\quad(3.2)$$

$$\mathrm{Re}\left[\delta u\frac{\partial\theta}{\partial x}+v\delta\frac{\partial\theta}{\partial y}\right]=\frac{1}{\mathrm{Pr}}\left[\delta^2\frac{\partial^2\theta}{\partial x^2}+\frac{\partial^2\theta}{\partial y^2}\right]+\beta+$$

$$M^2Eu^2+\frac{N^2\theta}{P_r}\quad(3.3)$$

Applying long wave length approximation and neglecting the wave number along with low-Reynolds numbers. Equations (10-12) become

$$\frac{\partial^2 u}{\partial y^2}-Au=\frac{\partial p}{\partial x}+A-\eta\sin\alpha\quad(3.4)$$

$$\frac{\partial p}{\partial y}=0\quad(3.5)$$

$$\frac{1}{\mathrm{Pr}}\left[\frac{\partial^2\theta}{\partial y^2}\right]+\beta+M^2Eu^2+\frac{N^2\theta}{P_r}=0\quad(3.6)$$

Where $A=\left(M^2+\frac{1}{Da}\right)$

The relative boundary conditions in dimensionless form are given by

$$u=-1,\quad \theta=0\quad\text{at}\quad y=h_1\quad(3.7)$$

$$u=-1,\quad \theta=1\quad\text{at}\quad y=h_2\quad(3.8)$$

Where

$$h_1=-1-k_1x-\varepsilon\sin\left[2\pi(x-t)+\phi\right]$$

$$h_2=1+k_1x+\varepsilon\sin\left[2\pi(x-t)\right]$$

Where β is the non-dimensional slip velocity parameter.

The solutions of velocity and temperature with subject to boundary conditions (3.7) and (3.8) are given by

$$u=f_1Sinh[\alpha y]+f_2Cosh[\alpha y]+F\quad(3.9)$$

Where

$$\alpha=\sqrt{\left(M^2+\frac{1}{Da}\right)}$$

$$F=\frac{-\frac{\partial p}{\partial x}}{M^2+\frac{1}{Da}}-1+\frac{\eta Sin\alpha}{M^2+\frac{1}{Da}}$$

$$f_1=\left(\frac{(-1-F)}{\left(\frac{Cosh[\alpha h_2]-Cosh[\alpha h_1]}{Sinh[\alpha h_1]-Sinh[\alpha h_2]}\right)Sinh[\alpha h_1]+Cosh[\alpha h_1]}\right)$$

$$\left(\frac{Cosh[\alpha h_2]-Cosh[\alpha h_1]}{Sinh[\alpha h_1]-Sinh[\alpha h_2]}\right)$$

$$f_2=\left(\frac{(-1-F)}{\left(\frac{Cosh[\alpha h_2]-Cosh[\alpha h_1]}{Sinh[\alpha h_1]-Sinh[\alpha h_2]}\right)Sinh[\alpha h_1]+Cosh[\alpha h_1]}\right)$$

$$\theta=f_9Cos[Ny]+f_8Sin[Ny]-\left(\frac{P_r\gamma}{N^2}\right)-\left(\frac{M^2B_rf_3}{4\alpha^2+N^2}e^{2\alpha y}\right)$$

$$-\left(\frac{M^2B_rf_4}{4\alpha^2+N^2}e^{-2\alpha y}\right)-\left(\frac{M^2B_rf_5}{\alpha^2+N^2}e^{\alpha y}\right)$$

$$-\left(\frac{M^2B_r f_6}{\alpha^2+N^2}e^{-\alpha y}\right)-\left(\frac{M^2B_r f_7}{N^2}\right) \quad (3.10)$$

Where

$$f_3=\left(\frac{f_1^{\,2}}{4}+\frac{f_2^{\,2}}{4}+\frac{f_1 f_2}{2}\right)$$

$$f_4=\left(\frac{f_1^{\,2}}{4}+\frac{f_2^{\,2}}{4}-\frac{f_1 f_2}{2}\right)\quad f_5=F(f_1+f_2)$$

$$f_6=F(f_2-f_1)\quad f_7=\left(\frac{-f_1^{\,2}}{2}+\frac{f_2^{\,2}}{2}+F^2\right)$$

$$f_8=\left(\frac{-\cos[N h_1]}{Sin[N h_1]\cos[N h_2]-Sin[N h_2]\cos[N h_1]}\right)-$$

$$\left(\frac{\left(\frac{P_r\gamma}{N^2}\right)(\cos[N h_1]-\cos[N h_2])}{Sin[N h_1]\cos[N h_2]-Sin[N h_2]\cos[N h_1]}\right)-$$

$$\left(\frac{\frac{M^2B_r f_3}{4\alpha^2+N^2}\left(e^{2\alpha h_2}\cos[N h_1]-e^{2\alpha h_1}\cos[N h_2]\right)}{Sin[N h_1]\cos[N h_2]-Sin[N h_2]\cos[N h_1]}\right)-$$

$$\left(\frac{\frac{M^2B_r f_4}{4\alpha^2+N^2}\left(e^{-2\alpha h_2}\cos[N h_1]-e^{-2\alpha h_1}\cos[N h_2]\right)}{Sin[N h_1]\cos[N h_2]-Sin[N h_2]\cos[N h_1]}\right)-$$

$$\left(\frac{\frac{M^2B_r f_5}{\alpha^2+N^2}\left(e^{\alpha h_2}\cos[N h_1]-e^{\alpha h_1}\cos[N h_2]\right)}{Sin[N h_1]\cos[N h_2]-Sin[N h_2]\cos[N h_1]}\right)-$$

$$\left(\frac{\frac{M^2B_r f_6}{\alpha^2+N^2}\left(e^{-\alpha h_2}\cos[N h_1]-e^{-\alpha h_1}\cos[N h_2]\right)}{Sin[N h_1]\cos[N h_2]-Sin[N h_2]\cos[N h_1]}\right)-$$

$$\left(\frac{\frac{M^2B_r f_7}{N^2}(\cos[N h_1]-\cos[N h_2])}{Sin[N h_1]\cos[N h_2]-Sin[N h_2]\cos[N h_1]}\right)$$

$$f_9=\left(\frac{-f_8 Sin[N h_1]+\left(\frac{P_r\gamma}{N^2}\right)+\frac{M^2B_r f_3}{4\alpha^2+N^2}\left(e^{2\alpha h_1}\right)}{\cos[N h_1]}\right)+$$

$$\left(\frac{\frac{M^2B_r f_4}{4\alpha^2+N^2}\left(e^{-2\alpha h_1}\right)+\frac{M^2B_r f_5}{\alpha^2+N^2}\left(e^{\alpha h_1}\right)}{\cos[N h_1]}\right)+$$

$$\left(\frac{\frac{M^2B_r f_6}{\alpha_1^{\,2}+N^2}\left(e^{-\alpha h_1}\right)+\frac{M^2B_r f_7}{N^2}}{\cos[N h_1]}\right)$$

The coefficients of the heat transfer Zh_1 and Zh_2 at the walls $y = h_1$ and $y = h_2$ respectively, are given by

$$Zh_1=\theta_y h_{1x} \quad (3.11)$$

$$Zh_2=\theta_y h_{2x} \quad (3.12)$$

The solutions of the coefficient of heat transfer at $y = h_1$ and $y = h_2$ are given by

$$Zh_1=\theta_y h_{1x}=$$

$$\left(-N f_9 Sin[Ny]+N f_8 Cos[Ny]-\left(\frac{2\alpha M^2B_r f_3}{4\alpha^2+N^2}e^{2\alpha y}\right)-\right.$$

$$\left.\left(\frac{-2\alpha M^2B_r f_4}{4\alpha^2+N^2}e^{-2\alpha y}\right)-\left(\frac{\alpha M^2B_r f_5}{\alpha^2+N^2}e^{\alpha y}\right)+\right.$$

$$\left(\frac{\alpha M^2 B_r f_6}{\alpha^2+N^2} e^{-\alpha y}\right)\Bigg)*$$

$$\left(-2\pi\varepsilon Cos\left[2\pi(x-t)+\phi\right]-k_1\right) \quad (3.13)$$

$$Zh_2 = \theta_y h_{2x} =$$

$$\left(-N f_9 Sin[Ny]+N f_8 Cos[Ny]-\left(\frac{2\alpha M^2 B_r f_3}{4\alpha^2+N^2} e^{2\alpha y}\right)-\right.$$

$$\left(\frac{-2\alpha M^2 B_r f_4}{4\alpha^2+N^2} e^{-2\alpha y}\right)-\left(\frac{\alpha M^2 B_r f_5}{\alpha^2+N^2} e^{\alpha y}\right)+$$

$$\left.\left(\frac{\alpha M^2 B_r f_6}{\alpha^2+N^2} e^{-\alpha y}\right)\right)*$$

$$\left(2\pi\varepsilon Cos[2\pi(-t+x)]+k_1\right) \quad (3.14)$$

The volumetric flow rate in the wave frame is defined by

$$q=\int_{h_1}^{h_2} u\,dy=\int_{h_1}^{h_2}(f_1 Sinh[\alpha y]+f_2 Cosh[\alpha y]+F)\,dy$$

$$\left(\frac{f_1}{\alpha}\right)(Cosh[\alpha h_2]-Cosh[\alpha h_1])+$$

$$\left(\frac{f_2}{\alpha}\right)(Sinh[\alpha h_2]-Sinh[\alpha h_1])+F(h_2-h_1) \quad (3.15)$$

The pressure gradient obtained from equation (3.15) can be expressed as

$$\frac{dp}{dx}=-A-A f_{12}+\eta Sin\alpha \quad (3.16)$$

Where

$$f_{10}=\left(\frac{(-1)}{\left(\frac{Cosh[\alpha h_2]-Cosh[\alpha h_1]}{Sinh[\alpha h_1]-Sinh[\alpha h_2]}\right)Sinh[\alpha h_1]+Cosh[\alpha h_1]}\right)*$$

$$\left(\frac{Cosh[\alpha h_2]-Cosh[\alpha h_1]}{Sinh[\alpha h_1]-Sinh[\alpha h_2]}\right)$$

$$f_{11}=\left(\frac{(-1)}{\left(\frac{Cosh[\alpha h_2]-Cosh[\alpha h_1]}{Sinh[\alpha h_1]-Sinh[\alpha h_2]}\right)Sinh[\alpha h_1]+Cosh[\alpha h_1]}\right)$$

$$f_{12}=\frac{q}{f_{13}}-\frac{\left(\frac{(Cosh[\alpha_1 h_2]-Cosh[\alpha_1 h_1])}{\alpha}\right)(f_{10})}{f_{13}}-$$

$$\frac{\left(\frac{(Sinh[\alpha_1 h_2]-Sinh[\alpha_1 h_1])}{\alpha}\right)(f_{10})}{f_{13}}$$

Where

$$f_{13}=\left(\frac{(Cosh[\alpha_1 h_2]-Cosh[\alpha_1 h_1])}{\alpha}\right)(f_{10})+$$

$$\left(\frac{(Sinh[\alpha_1 h_2]-Sinh[\alpha_1 h_1])}{\alpha}\right)(f_{10})+(h_2-h_1)$$

The instantaneous flux Q (x, t) in the laboratory frame is

$$Q=\int_{h_2}^{h_1}(u+1)dy=q-h \quad (3.17)$$

The average volume flow rate over one wave period (T = λ/c) of the peristaltic wave is defined as

$$\overline{Q}=\frac{1}{T}\int_0^T Q\,dt=q+1+d \quad (3.18)$$

From the equations (3.16) and (3.18), the pressure gradient can be expressed as

$$\frac{dp}{dx} = -A - A f_{14} + \eta Sin\alpha \qquad (3.19)$$

Where

$$f_{14} = \frac{(\bar{Q} - 1 - d)}{f_{13}} - \frac{\left(\frac{(Cosh[\alpha_1 h_2] - Cosh[\alpha_1 h_1])}{\alpha}\right)(f_{10})}{f_{13}} -$$

$$\frac{\left(\frac{(Sinh[\alpha_1 h_2] - Sinh[\alpha_1 h_1])}{\alpha}\right)(f_{10})}{f_{13}}$$

4. **Discussion of the problem**

Fig. 2 illustrates the variation in axial velocity for different values of the Hartman number M (M = 1, 1.5, 2) with fixed Da = 0.3, $\phi = \pi/6$, $\alpha = \pi/6$, $\eta = 0.5$, $\varepsilon = 0.2$, $k_1 = 0.1$, x = 0.6, t = 0.4, dp/dx = -0.5.We observe from this figure that the axial velocity diminished with increasing the values of Hartman number M. Fig. 3 depicts the variation in axial velocity for the variation in the porous parameter Da (Da = 0.1, 0.2, 0.3) with M = 1, $\phi = \pi/6$, $\alpha = \pi/6$, $\eta = 0.5$, $\varepsilon = 0.2$, $k_1 = 0.1$, x = 0.6, t = 0.4, dp/dx = -0.5. It shows that the axial velocity increases when the porosity parameter increases. The variation in axial velocity with different values of gravitational parameter η ($\eta = 0.1, 0.5, 1$) is shown in Fig. 4 with fixed M = 1, $\phi = \pi/6$, $\alpha = \pi/6$, $\eta = 0.5$, $\varepsilon = 0.2$, $k_1 = 0.1$, x = 0.6, t = 0.4, dp/dx = -0.5. We observe that an increasing the values of gravitational parameter η enhances the axial velocity. Fig. 5 displays the effect of non-uniform parameter k_1 ($k_1 = 0.1$, 0.2, 0.3) on the fluid velocity with fixed Da = 0.3, $\phi = \pi/6$, $\alpha = \pi/6$, M = 1, $\eta = 0.5$, $\varepsilon = 0.2$, x = 0.6, t = 0.4, dp/dx = -0.5. It can be seen from this figure that an increase in the value of non-uniform parameter k_1 results in a fluid velocity increases. Therefore, we conclude from these figures that the fluid velocity (See fig. 2-5) diminished when Hartmann number increased and also we notice that the fluid velocity enhances with increasing the values of Da, η and k_1.

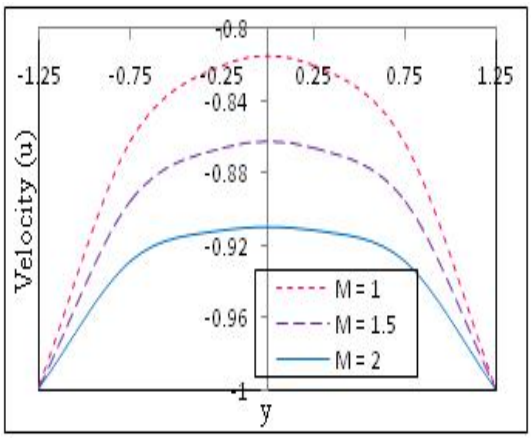

Figure (2): Velocity for different values of M with fixed Da = 0.3, $\phi = \pi/6$, $\alpha = \pi/6$,$\eta = 0.5$, $\varepsilon = 0.2$, $k_1 = 0.1$, x = 0.6, t = 0.4, dp/dx = -0.5.

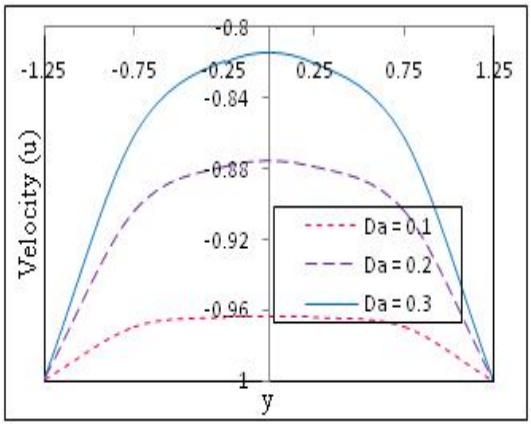

Figure (3): Velocity for different values of Da with fixed M = 1, $\phi = \pi/6$, $\alpha = \pi/6$,$\eta = 0.5$, $\varepsilon = 0.2$, $k_1 = 0.1$, x = 0.6, t = 0.4, dp/dx = -0.5.

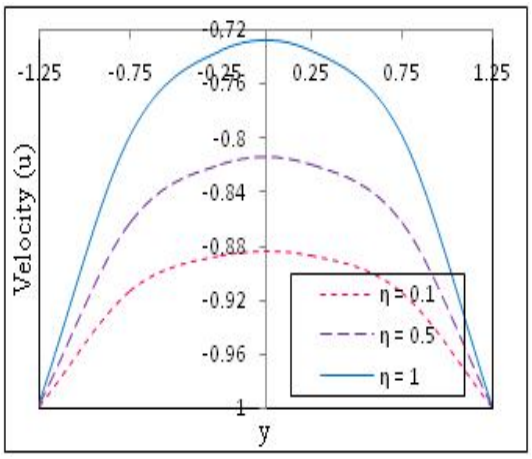

Figure (4): Velocity for different values of η with fixed Da = 0.3, ϕ = π/6, α = π/6,M = 1, ε = 0.2, k_1= 0.1, x = 0.6, t = 0.4, dp/dx = -0.5.

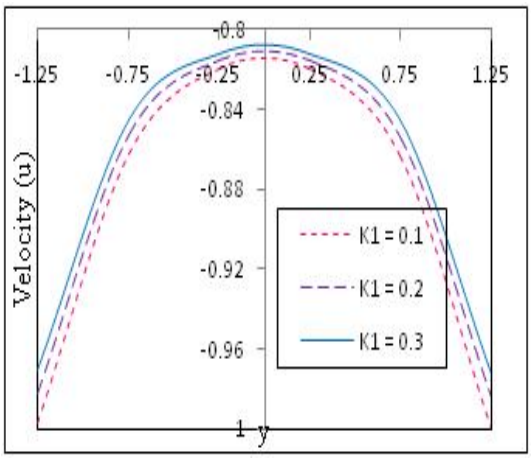

Figure (5): Velocity for different values of K_1 with fixed Da = 0.3, ϕ = π/6, α = π/6,M = 1, η = 0.5, ε = 0.2, x = 0.6, t = 0.4, dp/dx = -0.5.

Fig. 6 displays the effect of Hartmann number M on the pressure gradient with fixed other parameters Da = 0.3, ϕ = π/6, α = π/6, η = 0.5, ε = 0.2, k_1= 0.1, t = π/4, μ = 0.2, d = 2.It shows from this figure that the pressure gradient increases with increasing the values of Hartmann number M (M = 1, 1.5, 2). Fig. 7 illustrates that the porous parameter Da on pressure gradient with fixed M = 1, ϕ = π/6, α = π/6, η = 0.5, ε = 0.2, k_1= 0.1, t = π/4, μ = 0.2, d = 2. We notice that the pressure gradient diminishes when increase in porosity parameter Da. Influence of gravitational parameter η on pressure gradient is shown in fig. 8. This figure indicates the pressure gradient enhances when an increase in gravitational parameter η (η = 0.1, 0.5, 1) with fixed other parameters. Fig. 9 displays the effect of volumetric flow rate $\overline{Q}$ ($\overline{Q}$ = 0.2, 0.4, 0.6) on pressure gradient with fixed M = 1, ϕ = π/6, α = π/6, Da = 0.3, η = 0.5, ε = 0.2, k_1= 0.1, t = π/4, d = 2. It shows from this figure that an increase in volumetric flow rate μ results in pressure gradient diminished. Effect of non- uniform parameter k_1 on pressure gradient is presented in Fig.10.We observe that the pressure gradient decreases with increase in non –uniform parameter k_1 (k_1 = 0.1, 0.2, 0.3) with fixed M = 1, ϕ = π/6, α = π/6, Da = 0.3, η = 0.5, ε = 0.2, μ = 0.2, t = π/4, d = 2. An important result presented in Fig. 11. We notice from this figure that the pressure gradient decreases in the narrow part of the channel xε [0.5, 1] and here we require a lesser amount of pressure gradient to pass the flow in an asymmetric channel to the values of increase in ϕ. The pressure gradient increases in the wider part of the channel xε [0, 0.5] with increasing the values of ϕ. In the wider part of the channel, the flow cannot pass easily. Therefore, it required large pressure gradient to maintain the same flux to pass in the wider part of the channel.

$\overline{Q}$

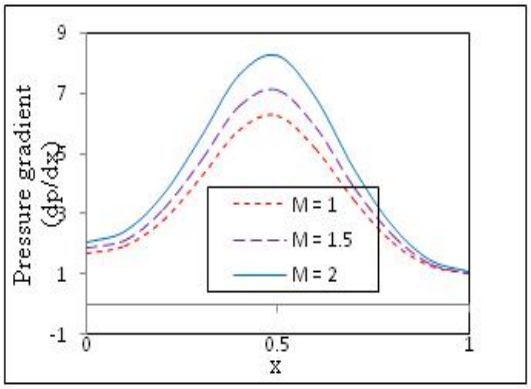

Figure (6): Pressure gradient (dp/dx) for different values of M with fixed Da = 0.3, $\phi = \pi/6$, $\alpha = \pi/6$, $\eta = 0.5$, $\varepsilon = 0.2$, $k_1 = 0.1$, $t = \pi/4$, $\mu = 0.2$, $d = 2$.

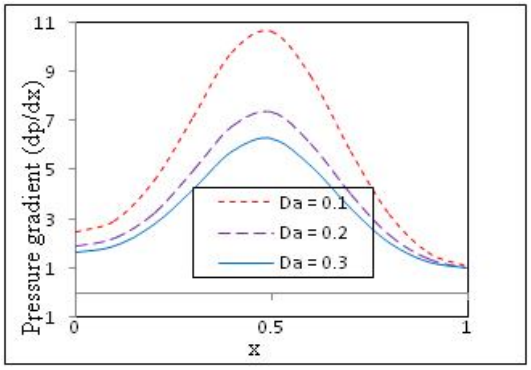

Figure (7): Pressure gradient (dp/dx) for different values of Da with fixed M = 1, $\phi = \pi/6$, $\alpha = \pi/6$, $\eta = 0.5$, $\varepsilon = 0.2$, $k_1 = 0.1$, $t = \pi/4$, $\mu = 0.2$, $d = 2$.

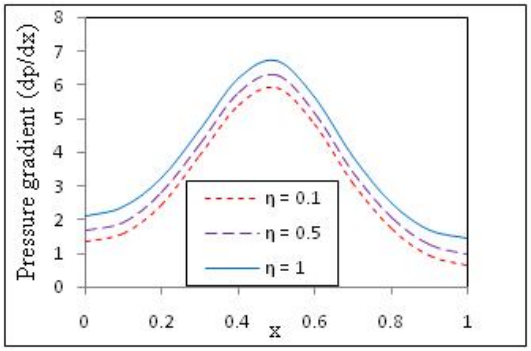

Figure (8): Pressure gradient (dp/dx) for different values of η with fixed M = 1, $\phi = \pi/6$, $\alpha = \pi/6$, Da = 0.3, $\varepsilon = 0.2$, $k_1 = 0.1$, $t = \pi/4$, $\mu = 0.2$, $d = 2$.

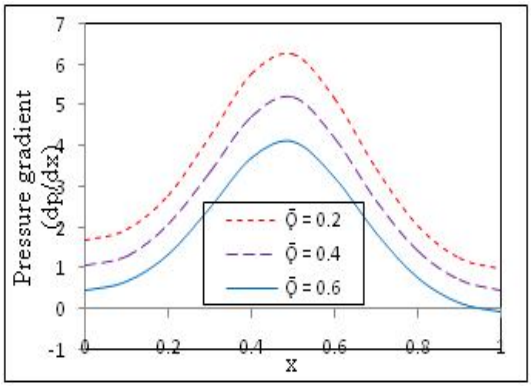

Figure (9): Pressure gradient (dp/dx) for different values of $\overline{Q}$ with fixed M = 1, $\phi = \pi/6$, $\alpha = \pi/6$, Da = 0.3, $\eta = 0.5$, $\varepsilon = 0.2$, $k_1 = 0.1$, $t = \pi/4$, $d = 2$.

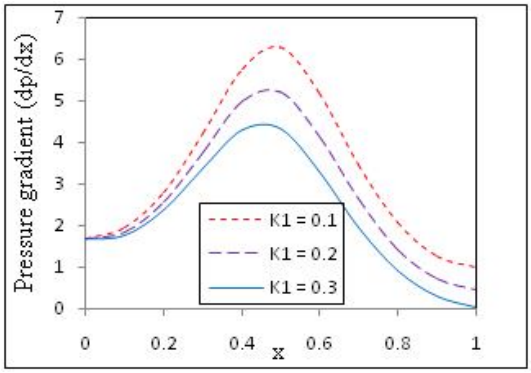

Figure (10): Pressure gradient (dp/dx) for different values of $\overline{Q}$ with fixed M = 1, $\phi = \pi/6$, $\alpha = \pi/6$, Da = 0.3, $\eta = 0.5$, $\varepsilon = 0.2$, $\mu = 0.2$, $t = \pi/4$, $d = 2$.

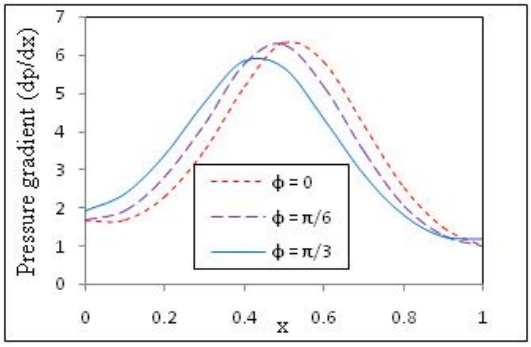

Figure (11): Pressure gradient (dp/dx) for different values of ϕ with fixed M = 1, $\alpha = \pi/6$, Da = 0.3, $\eta = 0.5$, $k_1 = 0.1$, $\varepsilon = 0.2$, $\mu = 0.2$, $t = \pi/4$, $d = 2$.

Influence of Hartmann number on temperature distribution (θ) is displayed in fig.12 with fixed Da = 0.3, N = 0.5, Pr =1, γ = 0.1, Br = 0.1, ϕ = π/6, α = π/6, η = 0.5, ε = 0.2, k_1= 0.1, x = 0.6, t = 0.4, p = 0.5. It was evident that the temperature distribution enhances when increase in Hartmann number M. Fig. 13 depicts the influence of porosity parameter Da on temperature distribution (θ) with fixed M = 1.5, N = 0.5, Pr =1, γ = 0.3, Br = 0.1, ϕ = π/6, α = π/6, η = 0.5, ε = 0.2, k_1= 0.1, x= 0.6, t = 0.4, p = 0.5. It has been inferred that the results in temperature of the fluid diminished as increase in porosity parameter Da (Da = 0.1, 0.2, 0.3) Fig. 14. Shows that the variation of radiation parameter on temperature distribution with M = 1, Da = 0.3, Pr =1, γ = 0.1, Br = 0.1, ϕ = π/6, α = π/6, η = 0.5, ε = 0.2, k_1= 0.1, x= 0.6, t = 0.4, p = 0.5.It could noted that the temperature distribution increases with increase in radiation parameter N (N = 0.5, 0.7, 0.9). Variation of Prandtl number Pr (Pr = 1, 3, 5) on temperature distribution has been plotted in Fig. 15. It was observe from graph that the temperature of the fluid enhances when increase in Prandtl number Pr with fixed other parameters. Fig.16. displays the effect of Brinkman number Br on temperature of the fluid (θ) with fixed M = 1, Da = 0.3, N = 0.5, γ = 0.1, Pr = 1, ϕ = π/6, α = π/6, η = 0.5, ε = 0.2, k_1= 0.1, x= 0.6, t = 0.4, p = 0.5. Indeed, the temperature of the fluid increases with increase in Brinkman number Br (Br = 0.1, 0.2, 0.3). Fig. 17 depicts to examine the effect of gravitational parameter η on temperature of the fluid with fixed M = 1, Da = 0.3, N = 0.5, γ = 0.1, Pr = 1, Br = 0.1, ϕ = π/6, α = π/6, ε = 0.2, k_1= 0.1, x= 0.6, t = 0.4, p = 0.5.This figure shows that the results in temperature of the fluid diminished as increase in gravitational parameter η (η = 0.1,0.5,1). Fig. 18 shows to examine the effect of heat source/sink parameter γ (γ = 0.1, 0.3, 0.5) on temperature distribution with M = 1, Da = 0.3, N = 0.5, η = 0.5, Pr = 1, Br = 0.1, ϕ = π/6, α = π/6, ε = 0.2, k_1= 0.1, x= 0.6, t = 0.4, p = 0.5.This figure shows that the temperature of the fluid enhanced with increasing the values of heat source/sink parameter γ.

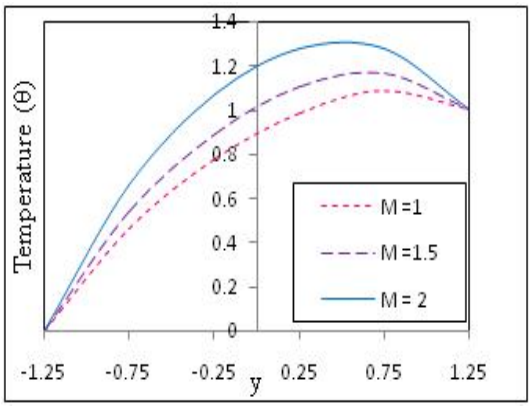

Figure (12): Temperature (θ) for different values of M with fixed Da = 0.3, N = 0.5, Pr =1, γ = 0.1, Br = 0.1, ϕ = π/6, α = π/6, η = 0.5, ε = 0.2, k_1= 0.1, x= 0.6, t = 0.4, p = 0.5.

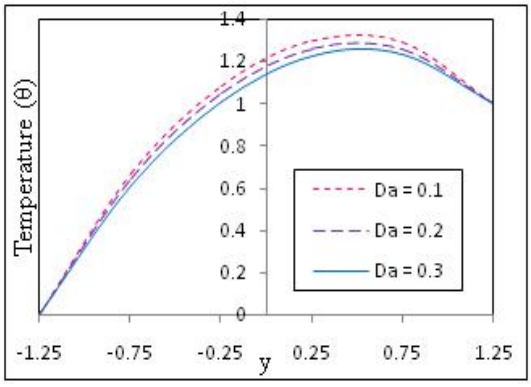

Figure (13): Temperature (θ) for different values of Da with fixed M = 1.5, N = 0.5,Pr =1, γ = 0.3, Br = 0.1, ϕ = π/6, α = π/6, η = 0.5, ε = 0.2, k_1= 0.1,x= 0.6, t = 0.4, p = 0.5.

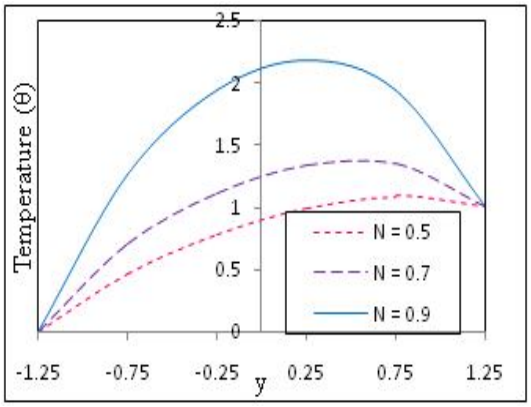

Figure (14): Temperature (θ) for different values of N with fixed M = 1, Da = 0.3,Pr =1, γ = 0.1, Br = 0.1, ϕ = π/6, α = π/6, η = 0.5, ε = 0.2, k_1 = 0.1,x= 0.6, t = 0.4, p = 0.5.

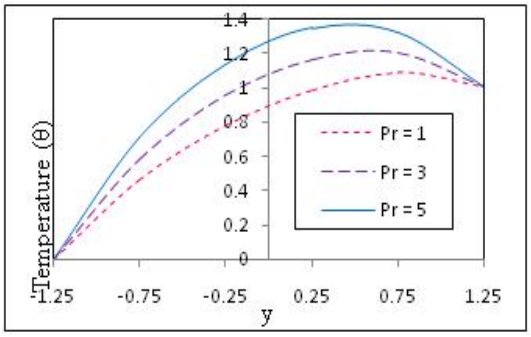

Figure (15): Temperature (θ) for different values of Pr with fixed M = 1, Da = 0.3, N = 0.5, γ = 0.1, Br = 0.1, ϕ = π/6, α = π/6, η = 0.5, ε = 0.2, k_1 = 0.1, x= 0.6, t = 0.4, p = 0.5.

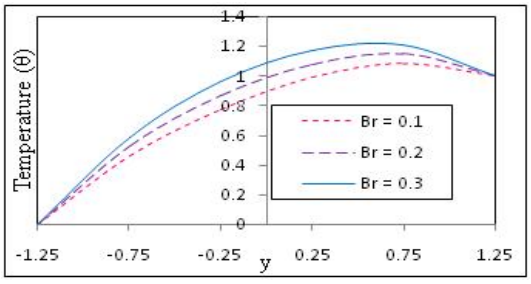

Figure (16): Temperature (θ) for different values of Br with fixed M = 1, Da = 0.3, N = 0.5, γ = 0.1, Pr = 1, ϕ = π/6, α = π/6, η = 0.5, ε = 0.2, k_1 = 0.1, x= 0.6, t = 0.4, p = 0.5.

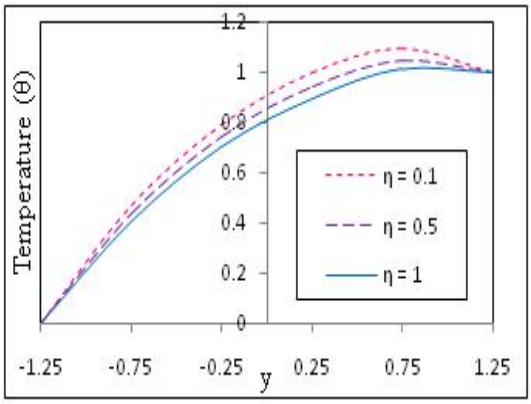

Figure (17): Temperature (θ) for different values of η with fixed M = 1, Da = 0.3, N = 0.5,γ = 0.1, Pr = 1, Br = 0.1, ϕ = π/6, α = π/6, ε = 0.2, k_1 = 0.1, x= 0.6, t = 0.4, p = 0.5.

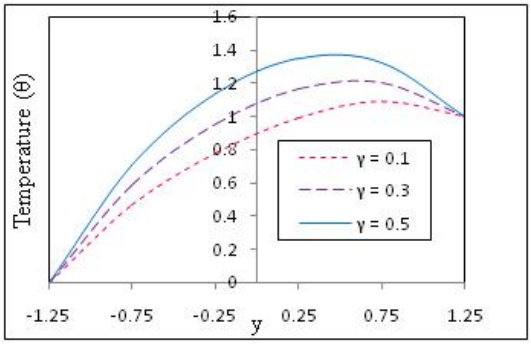

Figure (18): Temperature (θ) for different values of γ with fixed M = 1, Da = 0.3, N = 0.5, η = 0.5, Pr = 1, Br = 0.1, ϕ = π/6, α = π/6, ε = 0.2, k_1 = 0.1, x= 0.6, t = 0.4, p = 0.5.

Hartmann number M on heat transfer coefficient at the wall y = h_1 is presented in Fig. 19 with Da = 0.3, N = 0.5, Pr =1, γ = 0.1, Br = 0.1, ϕ = π/6, α = π/6, η = 0.5, ε = 0.2, k_1 = 0.1, t=0.4, p = 0.5. This figure reveals that the heat transfer coefficient increases in the portion of the inclined tapered channel x ε [0, 0.05] U [0.58, 1] and decreases in the other portion of the inclined tapered channel x ε [0.05, 0.58] with increase in M (M = 1, 1.5, 2). Fig. 20 shows

the effect of porosity parameter Da on heat transfer coefficient at the wall $y = h_1$ with M =1, N = 0.5, Pr =1, $\gamma = 0.1$, Br = 0.1, $\phi = \pi/6$, $\alpha = \pi/6$, $\eta = 0.5$, $\varepsilon = 0.2$, $k_1 = 0.1$, t = 0.4, p= 0.5.We observe from this figure that the results in the heat transfer coefficient is not significant in the entire inclined tapered channel. This may be due to the porosity parameter. We observe that the heat transfer coefficient gradually increases in part of the channel x ε [0.15, 0.5] and then decreases in the part of the channel x ε [0.5, 0.9] with increase in porosity parameter Da. Fig. 21 depicts to examine the effect of radiation parameter on heat transfer coefficient at the wall $y = h_1$ with M =1, Da = 0.3, Pr =1, $\gamma = 0.1$, Br = 0.1, $\phi = \pi/6$, $\alpha = \pi/6$, $\eta = 0.5$, $\varepsilon = 0.2$, $k_1 = 0.1$, t = 0.4, p= 0.5. We notice that the heat transfer coefficient increases in the portion of the portion channel x ε [0, 0.05] U [0.58, 1] and then decreases in the other portion of the channel x ε [0.05, 0.58] with increase in N (N = 0.5, 0.7, 0.9). Fig. 21 reveals the heat transfer coefficient at the wall $y = h_1$ with Prandtl number Pr being fixed M =1, Da = 0.3, N= 0.5, $\gamma = 0.1$, Br = 0.1, $\phi = \pi/6$, $\alpha = \pi/6$, $\eta = 0.5$, $\varepsilon = 0.2$, $k_1 = 0.1$, t = 0.4, p= 0.5.It can be notice that the heat transfer coefficient enhances in the portion of the channel x ε [0, 0.05] U [0.58, 1] and then diminished in the other portion of the channel x ε [0.05, 0.58] with increasing the values of Prandtl number Pr (Pr = 1, 3, 5). Fig. 23 illustrates the variation in heat transfer coefficient at the wall $y = h_1$ with Brinkman number Br being fixed M =1, Da = 0.3, N= 0.5, Pr =1, $\gamma = 0.1$, $\phi = \pi/6$, $\alpha = \pi/6$, $\eta = 0.5$, $\varepsilon = 0.2$, $k_1 = 0.1$, t = 0.4, p= 0.5. This figure indicates that the heat transfer coefficient enhances in the portion of the inclined tapered channel x ε [0, 0.05] U [0.58, 1] and then diminished in the rest of the inclined tapered channel x ε [0.05, 0.58] when increase Brinkman number Br (Br = 0.1,0.2,0.3). Influence of gravitational parameter η on heat transfer coefficient at the wall $y = h_1$ is presented in fig. 24 with fixed M =1, Da = 0.3, N= 0.5, Pr =1, Br = 0.1, $\gamma = 0.1$, $\phi = \pi/6$, $\alpha = \pi/6$, $\varepsilon = 0.2$, $k_1 = 0.1$, t = 0.4, p= 0.5.It can be notice that the heat transfer coefficient enhances in the portion of the channel x ε [0.05, 0.58] and then diminished in the portion of the x ε [0.58, 1] with increase in gravitational parameter η. Fig. 25 reveals the variation in heat transfer coefficient at the wall $y = h_1$ with heat source/sink parameter γ (γ = 0.1, 0.3, 0.5) being fixed M =1, Da = 0.3, N= 0.5, Pr =1, Br = 0.1, η = 0.5, $\phi = \pi/6$, $\alpha = \pi/6$, $\varepsilon = 0.2$, $k_1 = 0.1$, t = 0.4, p= 0.5. We notice from this figure that the results in heat transfer coefficient enhances in the portion of the inclined tapered channel x ε [0, 0.05] U [0.58, 1] and then diminished in the rest of the inclined tapered channel x ε [0.05, 0.58] when increase in heat source/sink parameter γ.

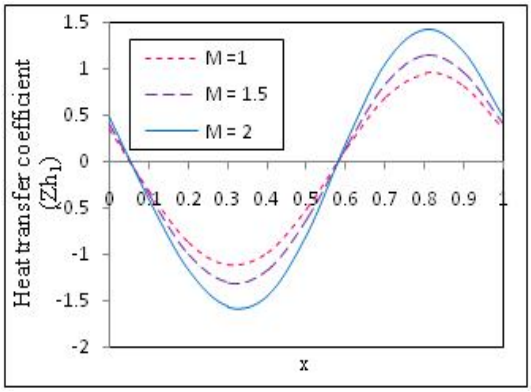

Figure (19): Heat transfer coefficient ($y = h_1$) for different values of M with fixed Da = 0.3, N = 0.5, Pr =1, $\gamma = 0.1$, Br = 0.1, $\phi = \pi/6$, $\alpha = \pi/6$, $\eta = 0.5$, $\varepsilon = 0.2$, $k_1 = 0.1$, t = 0.4, p= 0.5.

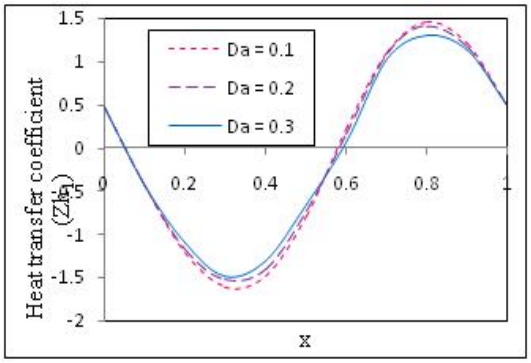

Figure (20): Heat transfer coefficient ($y = h_1$) for different values of Da with fixed M =1,N = 0.5, Pr =1, $\gamma = 0.1$, Br = 0.1, $\phi = \pi/6$, $\alpha = \pi/6$, $\eta = 0.5$, $\varepsilon = 0.2$, $k_1 = 0.1$, t = 0.4, p= 0.5.

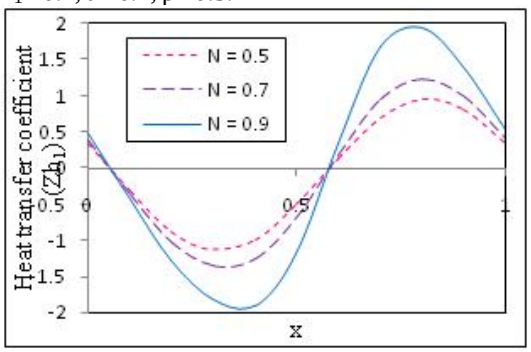

Figure (21): Heat transfer coefficient ($y = h_1$) for different values of N with fixed M =1, Da = 0.3, Pr =1, $\gamma = 0.1$, Br = 0.1, $\phi = \pi/6$, $\alpha = \pi/6$, $\eta = 0.5$, $\varepsilon = 0.2$, $k_1 = 0.1$, t = 0.4, p= 0.5.

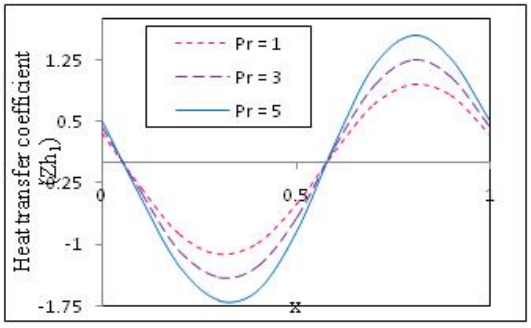

Figure (22): Heat transfer coefficient ($y = h_1$) for different values of N with fixed M =1, Da = 0.3, N= 0.5, $\gamma = 0.1$, Br = 0.1, $\phi = \pi/6$, $\alpha = \pi/6$, $\eta = 0.5$, $\varepsilon = 0.2$, $k_1 = 0.1$, t = 0.4, p= 0.5.

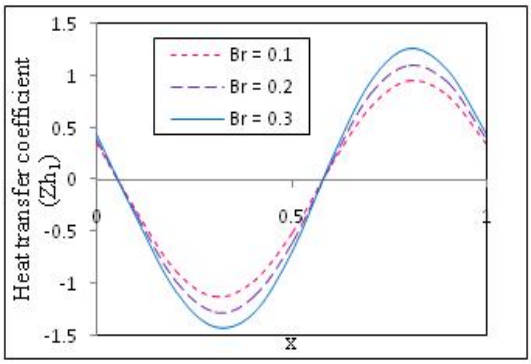

Figure (23): Heat transfer coefficient ($y = h_1$) for different values of N with fixed M =1, Da = 0.3, N= 0.5, Pr =1, $\gamma = 0.1$, $\phi = \pi/6$, $\alpha = \pi/6$, $\eta = 0.5$, $\varepsilon = 0.2$, $k_1 = 0.1$, t = 0.4, p= 0.5.

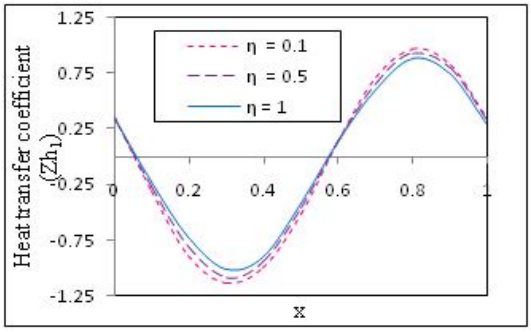

Figure (24): Heat transfer coefficient ($y = h_1$) for different values of η with fixed M =1, Da = 0.3, N= 0.5, Pr =1, Br = 0.1, $\gamma = 0.1$, $\phi = \pi/6$, $\alpha = \pi/6$, $\varepsilon = 0.2$, $k_1 = 0.1$, t = 0.4, p= 0.5.

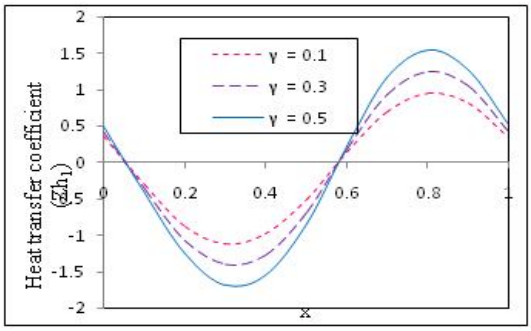

Figure (25): Heat transfer coefficient ($y = h_1$) for different values of η with fixed M =1, Da = 0.3, N= 0.5, Pr =1, Br = 0.1, $\eta = 0.5$, $\phi = \pi/6$, $\alpha = \pi/6$, $\varepsilon = 0.2$, $k_1 = 0.1$, t = 0.4, p= 0.5.

Conclusions

In this paper, we have proposed a theoretical study of ananalysis of joule heating and radiation on hydromagnetic peristalticflow with porous medium through a coaxial asymmetric vertical inclined tapered channel. The study has paid a special attention to examining the effects of Hartmann number, porosity parameter, volumetric flow rate, radiation parameter, non-uniform parameter, gravitational parameter, shift angle, Prandtl number, Brinkman number, heat source/sink parameter on the flow characteristics. We have concluded the following key observations:

(1) The axial velocity increases with increase in porosity parameter Da, gravitational parameter η and non-uniform parameter k1.
(2) The axial velocity diminished with increase in Hartmann number M.
(3) Pressure gradient enhances with an increase in Hartmann number M and gravitational parameter η.
(4) Pressure gradient diminished with increase in porosity parameter Da, non-uniform parameter k1and volumetric flow rate $\overline{Q}$.
(5) The temperature of the fluid enhances with an increase in Hartmann number M, radiation parameter N, Prandtl number Pr, Brinkman number Br and heat source/sink parameter γ.
(6) The temperature of the fluid diminished with increase in porosity parameter Da and gravitational parameter η.
(7) Heat transfer coefficient increases in the portion of the inclined tapered channel x ε [0, 0.05] U [0.58, 1] and decreases in the other portion of the inclined tapered channel x ε [0.05, 0.58] with increase in Hartmann number M, radiation parameter N, Prandtl number Pr, Brinkman number Br and heat source/sink parameter γ.
(8) Heat transfer coefficient gradually increases in part of the channel x ε [0.15, 0.5] and then decreases in the part of the channel x ε [0.5, 0.9] with an increase in porosity parameter Da.
(9) Heat transfer coefficient enhances in the portion of the channel x ε [0.05, 0.58] and then diminished in the portion of the x ε [0.58, 1] with an increase in gravitational parameter η.

References

1. Latham T.W. Fluid Motion in a Peristaltic Pump, MSc Thesis, Massachusetts Institute of Technology, Cambridge, Massachusetts, (1966).
2. Fung Y.C. and Yih, C.S. Peristaltic Transport, *J. Appl. Mech., 35,* 669-675 (1968).
3. Shapiro A.M., Jaffrin, M.Y. and Weinberg, S.L. Peristaltic Pumping with Long Wavelengths at Low Reynolds Number, *J. Fluid Mechanics, 37,* 799-825(1969).
4. M. Mishra M., Rao A. R. Peristaltic transport of a Newtonian fluid in an asymmetric channel, *Z. Angew Math. Phys. 54,* 440-532 (2004).
5. Hayat T., Rija Iqbal, Anum Tanveer, Alsaedi A. Influence of convective conditions in radiative peristaltic flow of pseudoplastic nanofluid in a tapered asymmetric channel, *Journal of Magnetism and Magnetic Materials. 408,* 168–176 (2016).
6. Abbasi F.M., Hayat T. and Alsaedi A. Numerical Analysis for Peristaltic Motion of MHD Eyring-Prandtl Fluid in an Inclined Symmetric Cannel with Inclined Magnetic Field, *Journal of Applied Fluid Mechanics. 9(1),* 389-396 (2016).
7. Mekheimer Kh.S. Peristaltic transport of a Newtonian fluidthrough a uniform and

non-uniform annulus, *Arab. J. Sci. Eng. 30 (1A)* 69–83 (2005).

8. Misra J.C., Maiti S. and Shit G.C. Peristaltic transport of aphysiological fluid in an asymmetric porous channel in thepresence of an external magnetic field, *J. Mech. Med. Biol. 8 (4),* 507–525 (2008).
9. Haroun M.H. Non linear peristaltic flow of a fourth grade fluid in an inclined asymmetric channel, *Comput. Mater. Sci. 39,* 324–333 (2007).
10. Akbar N.S., Hayat T., Nadeem S. and Obaidat S. Peristaltic flow of a Williamson fluid in an inclined asymmetric channel with partial slip and heat transfer, *Int. J. Heat Mass Transf. 55,* 1855–1862 (2012).
11. Sarkar B.C., Das S., Jana R.N. and Makinde O. D. Magnetohydrodynamic peristaltic flow of nanofluids in a convectively heated vertical asymmetric channel in presence of thermal radiation, *J. Nanofluids. 4 (4),* 461–473 (2015).
12. Ravikumar S. and Siva Prasad R. Interaction of pulsatile flow on the peristaltic motion of couple stress fluid through porous medium in a flexible channel, Eur. *J. Pure Appl. Math. 3,* 213-226 (2010).
13. Ravikumar S. Peristaltic transportation with effect of magnetic field in a flexible channel under an oscillatory flux, *Journal of Global Research in Mathematical Archives. 1(5),* 53-62 (2013).
14. Ravikumar S. Peristaltic flow of blood through coaxial vertical channel with effect of magnetic field: Blood flow study, *International Journal of Recent advances in Mechanical Engineering* (IJMECH). *3(4),* 85-96 (2014).
15. Kabir K. H., Alim M. A. and Andallah L.S. Effects of stress work on MHD natural convection flow along a vertical wavy surface with Joule heating, *Journal of Applied Fluid Mechanics, 8,* 213-221 (2015).
16. Hayat T., Farooq S., Ahmad B. and Alsaedi A. Characteristics of convective heat transfer in the MHD peristalsis of Carreau fluid with Joule heating, AIP Advances. 6, 045302 (2016).
17. Abbasi F.M., Hayat T. and Alsaedi A. Effects of inclined magnetic field and Joule heating in mixed convective peristaltic transport of non-Newtonian fluids, *Bulletin of the polish academy of sciences technical sciences. 63(2),* (2015).
18. Ravikumar S. Analysis of Heat Transfer on MHD Peristaltic Blood Flow with Porous Medium through Coaxial Vertical Tapered Asymmetric Channel with Radiation – Blood Flow Study, *International Journal of Bio-Science and Bio-Technology. 8(2),* 395-408 (2016).
19. Nadeem S. and Noreen Sher Akbar. Effects of heat transfer on the peristaltic transport of MHD Newtonian fluid with variable viscosity: Application of Adomian decomposition method, *Commun Nonlinear Sci. Numer Simulat. 14,* 3844-3855 (2009).
20. Hayat T., Najma Saleem, Asghar S., Mohammed Shabab Alhothuali and Adnan Alhomaidan. Influence of induced magnetic field and heat transfer on peristaltic transport of a Carreau fluid, *Commun Nonlinear Sci. Numer Simulat. 16,* 3559-3577 (2011).
21. Vajravelu K., Sreenadh S. and

Lakshminarayana P. The influence of heat transfer on peristaltic transport of a Jeffrey fluid in a vertical porous stratum, *Commun Nonlinear Sci Numer Simulat. 16,* 3107-3125 (2011).

22. Srinivas S. and Kothandapani M. Peristaltic transport in an asymmetric channel with heat transfer - A note, International *Communications in Heat and Mass* Transfer. *35,* 514-522 (2008).
23. Hayat T. Humaira Yasmina and Maryem Al- Yami. Soret and Dufour effects in peristaltic transport of physiological fluids with chemical reaction: *A mathematical analysis, Computers and Fluids. 89,* 242-253 (2014).
24. Mehmood O.U., Mustapha N. and Shafie S. Heat transfer on peristaltic flow of fourth grade fluid in inclined asymmetric channel with partial slip, *Appl. Math. Mech. - Engl. Ed. 33(10),* 1313-1328 (2012).
25. Musharafa Saleem and Aun Haider. Heat and mass transfer on the peristaltic transport of non-Newtonian fluid with creeping flow, International *Journal of Heat and Mass Transfer. 68,* 514-526 (2014).
26. G. Radhakrishnamacharya, Ch. Srinivasulu, Influence of wall properties on peristaltic transport with heat transfer, CR Mecanique, *335,* 369-373 (2007).
27. Vajravelu K., Radhakrishnamacharya G. and Radhakrishnamurty V. Peristaltic flow and heat transfer in a vertical porous annulus with long wavelength approximation, *Int. J. Nonlinear Mech. 42,* 754-759 (2007).
28. Ramesh K. and Devakar M., Magnetohydrodynamic peristaltic transport of couple stress fluid through porous medium in an inclined asymmetric channel with heat transfer, *J. Magn. Magn. Mater. 394,* 335–348 (2015).
29. Kothandapani, M., Pushparaj, V. and Prakash, J. On Effects of Slip and Heat Transfer on the MHD Peristaltic Flow of a Jeffery Fluid through a Vertical Tapered Asymmetric Channel, *Global Journal of Pure and Applied Mathematics* (GJPAM). *12(1),* 205-212 (2016).
30. Abzal S.K., Vijaja Kumar Varma S. and Ravikumar S. influence of heat transfer on magnetohydrodynamic peristaltic blood flow with porous medium through a coaxial vertical asymmetric tapered channel - an analysis of blood flow study, International *Journal of Engineering Sciences & Research Technology. 5(4),* 896-915 (2016).
31. Cogley A.C.L., Vinvent W.G. and Giles E.S. Differential approximation for radiative heat transfer in non-linear equations-grey gas near equilibrium, *American Institute of Aeronautics and Astronautics. 6,* 551–553 (1968).